

Supporting Information

**Self-assembly of artificial sweetener aspartame adversely affect phospholipid membranes:
plausible reason for its deleterious intake**

Sourav Nandi, Souvik Layek, Pratyush Kiran Nandi, Nanigopal Bera, Ritwik Hazra and Nilmoni Sarkar*

Department of Chemistry, Indian Institute of Technology Kharagpur, WB, 721302, India

E-mail: nilmoni@chem.iitkgp.ac.in and nilmonisarkar1208@gmail.com

Fax: 91-3222-255303

Table of contents

1. Materials and sample preparation.....	S2-S3
2. Instrumentations	S3-S7
3. Experimental protocols.....	S7-S9
4. Supporting tables.....	S10-S12
5. Supporting figures	S12-S19
6. References.....	S19-S20

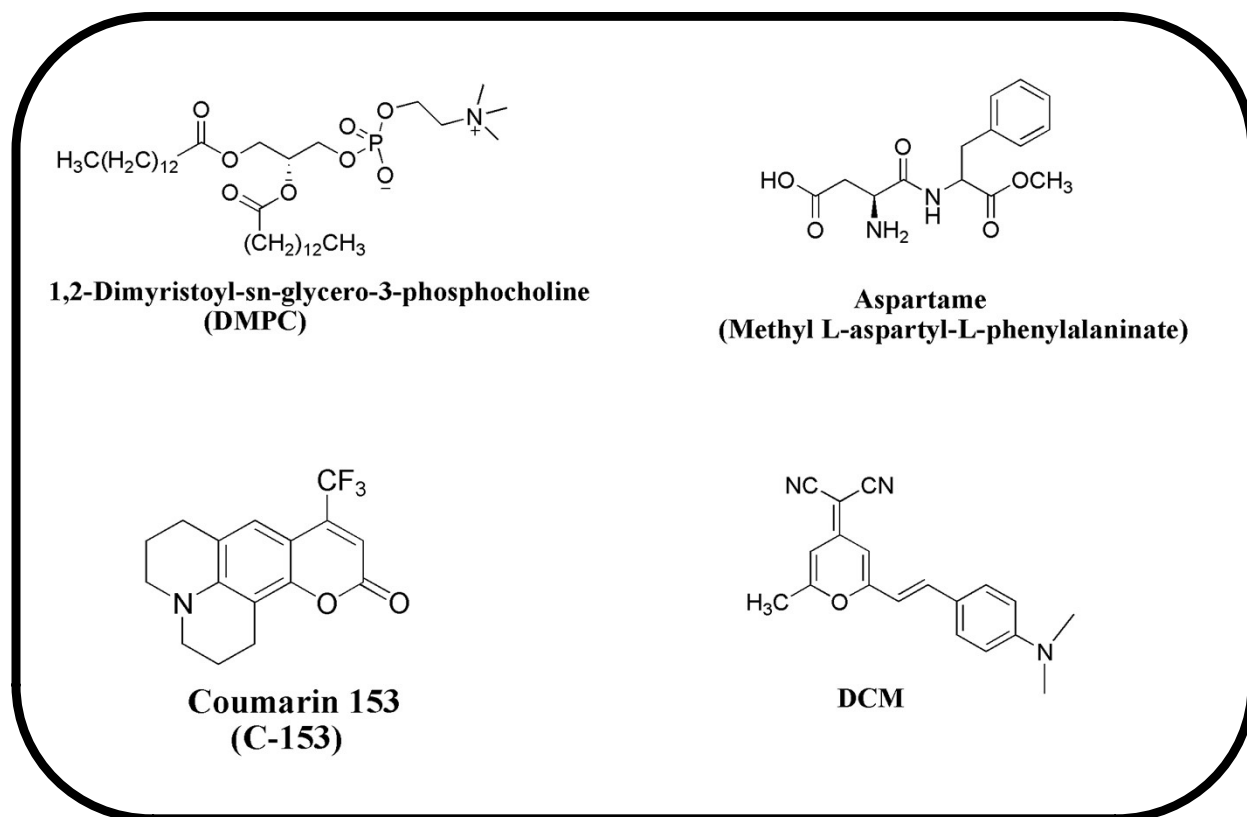
1. Materials and Sample Preparation:

The phospholipid 1,2-dimyristoyl-sn-glycero-3-phosphocholine (DMPC) was purchased from Sigma-Aldrich. Aspartame was ordered from TCI Chemicals (India) Pvt. Ltd. Coumarin 153 (C-153), 4-(Dicyanomethylene)-2-methyl-6-(4-dimethylaminostyryl)-4H-pyran (DCM) were obtained from Exciton to perform various steady-state as well as time-resolved spectroscopic experiments. The chemical structures of these materials are shown in **Scheme 1**. All of the experiments were performed at room temperature (298 K).

To prepare the solutions, double-distilled water having room temperature resistivity of 18.2 M Ω .cm was used throughout the study unless otherwise mentioned. The stock solution of aspartame was prepared in phosphate buffer saline (PBS, 0.1 M, pH 7.4). The solution of the lipid membrane was prepared by dissolving a pre-weighed powder of lipids in the 1:1 (v/v) solvent mixture of chloroform and methanol in a 10 ml round bottom flask to a final concentration of 3 mM. This solution was then evaporated completely employing a rotary evaporator, followed by keeping the flask in the vacuum desiccators overnight, which leaves a lipid layer at the bottom of the flask. The lipid film was dissolved with PBS at 298 K to prepare a solution of multilamellar lipid vesicles (MLV), followed by the preparation of unilamellar vesicles through probe sonication with a probe sonicator (Processor SONOPROS PR-250 MP, Oscar Ultrasonics Pvt. Ltd. India) having an operating frequency of $\sim 20 \pm 3$ kHz for 10 minutes. The specification of the probe sonicator performing the sonication cycle was as follows- extreme power 130 W, operating frequency $\sim 20 \pm 3$ kHz, sonotrode tip length ~ 6 cm. Within these 10 minutes of total time, several cycles were operated. Specifically, one mL of the solution was taken in the eppendorf, and subjected to ultrasound application for three seconds followed by a time lag of five seconds. During the time lag, the ultrasound applicator remains turned off to prevent the sample from thermal degradation. However, this was followed by the centrifugation of the vesicle solution using microcentrifuge (SPINWIN from TARSON, model number- MC02) with 10000 rpm for five minutes to remove the titanium particles added during the sonication, as mentioned earlier. The supernatant obtained was transferred to a fresh eppendorf and used for further experimentation. This supernatant was further passed through the 450 nm pore size cellulose filter paper to get uniformly distributed vesicles having average size ~ 100 nm vesicles.

For spectroscopic measurement, we have used the sonicated vesicles of size ~ 100 nm, whereas for microscopic investigation, we used unsonicated $\sim \mu\text{m}$ sized vesicles.

Scheme 1. Structures of the chemicals used in this study: 1,2-Dimyristoyl-sn-glycero-3-phosphocholine (DMPC), Aspartame (Methyl L-aspartyl-L-phenylalanine), Coumarin 153 (C-153), 4-(Dicyanomethylene)-2-methyl-6-(4-dimethylaminostyryl)-4H-pyran (DCM)



2. Instrumentations:

2.1. Dynamics Light Scattering (DLS)

Dynamic light scattering (DLS) measurements were performed using a Malvern Nano ZS instrument employing a 4 mW He–Ne laser ($\lambda = 632.8$ nm) and equipped with a thermostatic sample chamber and the detector angle was fixed at 173° . The same instrument was used to measure the zeta potentials of various solutions presented in the manuscript.

2.2. Fluorescence Correlation Spectroscopy (FCS)

In FCS, a very small observation volume (typically of an order of femtolitre) was created inside the sample using DCS 120 confocal laser scanning microscope (LSM) system (Becker & Hickl DCS 120) equipped with an inverted optical microscope of Zeiss (Carl Zeiss, Germany) and a 40X water emulsion objective (NA = 1.2). The Picosecond diode laser of 488 nm was used as an excitation source, and the sample was placed onto a glass coverslip. Due to the diffusion of the fluorescence molecules in and out of the observed volume,¹ the fluctuations in fluorescence intensity was time-correlated to form a normalized auto-correlation function, $G(\tau)$ which may be expressed as^{2,3} -

$$G(\tau) = \frac{\langle \delta F(t)\delta F(t + \tau) \rangle}{\langle F(t)^2 \rangle} \quad (2)$$

Where $\delta F(t)$ and $\delta F(t + \tau)$ signifies the amounts of intensity fluctuation around at time t and $t + \tau$ respectively, τ indicates the delay and $\langle F(t) \rangle$ denotes average fluorescence intensity.

$$\delta F(t) = F(t) - \langle F(t) \rangle \quad (3)$$

$$\delta F(t + \tau) = F(t + \tau) - \langle F(t + \tau) \rangle \quad (4)$$

A 3D diffusion model was used to fit the autocorrelation traces so obtained.

For n fraction of dyes diffusing within the system having distinct coefficients, $G(\tau)$ may be defined as, (5)

$$G(\tau) = \frac{1}{N} \sum_{i=1}^2 A_i \left(\frac{1}{1 + \left(\frac{\tau}{\tau_D^i}\right)} \right) \left(\frac{1}{1 + \frac{1}{\omega^2} \left(\frac{\tau}{\tau_D^i}\right)} \right)^{1/2}$$

Where N stands for the number of dye molecules within the observed volume, A_i is the fractional weighting factor for the i^{th} contribution to the autocorrelation curve, and τ_D^i denotes the diffusion time of the dye molecules, and τ indicates delay time or lag time. The structure parameter (ω) is the ratio of longitudinal radii (l) to transverse radii (r), where r is related to diffusion coefficient (D_i) by the following equation,

$$D_{t=} \frac{r^2}{4\tau_D} \quad (6)$$

Here τ_D is the diffusion time of the probe molecule within the observed volume. In FCS measurement, it is customary to perform a calibration procedure where the confocal volume, as well as the structural parameter (ω) is determined using a reference dye before determining the correct diffusion coefficients for the sample of own interest.⁴

Here we have used Rhodamine 6G (R6G) as reference fluorescence probe of the known diffusion coefficient in water ($D_t = 426 \mu\text{m}^2 \text{s}^{-1}$), and the structural parameter (ω) of the confocal volume was obtained applying the following equation-

$$G(\tau) = \frac{1}{N} \left(1 + \frac{4D_t\tau}{r^2}\right)^{-1} \left(1 + \frac{4D_t\tau}{\omega^2 r^2}\right)^{-\frac{1}{2}} \quad (7)$$

The correlation trace of R6G in water was fitted, keeping r and ω as linked global parameters. This provides the value of ω as 5. The estimation of the observed volume was valued using the following equation,

$$V_{eff} = \pi^{\frac{3}{2}} \omega_{xy}^3 \omega \quad (8)$$

This estimates the value of V_{eff} as 1.35 fl with a transverse radius of 365 nm.

In general, the ensemble-averaged mean square displacements (MSD) i.e., $\langle r^2(t) \rangle = 6D_t t$ is contemplated as a characteristic of diffusion, where D_t stands for normal time-dependent Stoke-Einstein diffusion constant, and this type of diffusion is known as Fickian diffusion.⁵

2.3. Fluorescence Lifetime Imaging Microscopy (FLIM)

Fluorescence Lifetime Imaging Microscopy (FLIM) is a very sensitive tool to extract molecular level information of various large-sized molecular aggregates. Our instrument is composed of a laser scanning confocal FLIM microscope (Becker & Hickl DCS-120) equipped with an inverted optical microscope of Zeiss controlled by a galvodrivel unit (Becker & Hickl GDA- 120). Lifetime images were collected using DCS 120 fitted with a polarizing beam splitter and two

avalanche photodiode detectors (ID-Quantique ID100). Here the sample solutions were excited by a 488 nm diode laser operating at pulse mode (10 mW, a repetition rate of 50 MHz), and the fluorescence signal was separated from the excitation source using long pass filters (498 nm). The lifetime images presented in the manuscript are collected with the help of polarized fluorescence transient obtained by time-correlated single photon counting detection electronics (Becker & Hickl SPC-152, PHD-400-N reference diode),⁶ and the corresponding intensity images were obtained from the photons in all time channels of the pixels. The instrument response function of this system is less than 100 ps fwhm (full width half maximum).

2.4. Steady-State and Time-Resolved Fluorescence Studies

To perform the fluorescence measurements, DCM and C-153 were used as fluorescence dyes, which were excited at 488 nm and 405 nm respectively. The steady-state fluorescence emission was recorded using Hitachi (model number F- 7000) spectrofluorimeter. On the other hand, the time-resolved fluorescence emission decays of C-153 in the vesicle solutions containing various concentrations of ASP were recorded by the picosecond time-correlated single photon counting (TCSPC) set up. An instrumentation detail of this TCSPC setup is mentioned elsewhere.¹⁹ Briefly, picosecond diode laser (IBH, UK, Nanoled; 408 nm) was used as excitation source, and the emission decays were detected at magic angle (54.7°) polarisation using Hamamatsu microchannel plate photomultiplier tube (MCP PMT) (3809U) detector. The time-resolved decays were analyzed using IBH DAS-6 decay analysis software. The estimated instrument response function (IRF) of this TCSPC set-up is ~100 ps.

To study the solvation dynamics, it is customary to construct time-resolved emission spectra (TRES) using best fit parameters of the emission decays along with the steady-state emission spectra of the probe, as described by Fleming and Maroncelli.⁷ This solvation dynamics process is usually expressed by solvent correlation function, $C(t)$, which is designated as

$$C(t) = \frac{\nu(t) - \nu(\infty)}{\nu(0) - \nu(\infty)} \quad (9)$$

Where $\nu(0)$ denotes peak frequency at zero time, $\nu(t)$ at time t and $\nu(\infty)$ at infinite time. The decays obtained for $C(t)$ can be fitted applying the following multi-exponential function-

$$C(t) = \sum_i^n a_i \exp(-t/\tau_i) \quad (10)$$

The average solvation time ($\langle \tau_s \rangle$) can be estimated employing the equation-

$$\langle \tau_s \rangle = \sum_i^n a_i \tau_i \quad (11)$$

a_i in the above equations indicate relative amplitude of solvation, and τ_i stands for corresponding solvation times.

Furthermore, the reference picosecond TCSPC setup was used to record the anisotropy decays of C-153 in the vesicle solutions. The essential technicality of this measurement is the usage of vertically polarised light as excitation source, and a motorized polariser at the emission side to record the emission decays at parallel, $I_{||}(t)$ and perpendicular, $I_{\perp}(t)$ polarizations provided a particular peak difference between $I_{||}(t)$ and $I_{\perp}(t)$ decays were obtained. The anisotropy decay function, $r(t)$ is represented as⁸

$$r(t) = \frac{I_{||}(t) - GI_{\perp}(t)}{I_{||}(t) + 2GI_{\perp}(t)} \quad (12)$$

Where, G stands for correction factor and for our instrument the value is 0.6

3. Experimental protocols

3.1. Cell culture and cell viability assay protocol

3T3 mouse embryonic fibroblast cells were used between 10-15 passages. Cells were maintained in DMEM-high glucose (AT007, Himedia) supplemented with 10% foetal bovine serum (RM1112, Himedia) and 1% antibiotic-antimycotic solution (A002A, Himedia) in a cell-culture incubator at 37 °C and 5% CO₂. For cell viability, 3-(4, 5-dimethylthiazolyl-2)-2, 5-diphenyltetrazolium bromide (MTT) assay was performed. For MTT assay, about 3×10^3 cells were seeded in the wells of a 96-well plate. Cells were allowed to adhere and grow in the wells for 24 hours after which the sample of aspartame were added in concentrations 1.2, 2, and 5 mM. Only a complete DMEM medium was added in positive control wells. 100% DMSO was added

to the negative control wells. Appropriate no-cell blanks were taken for each of the treatment and control groups. The cells were maintained under treatment for 24 hours in the cell-culture incubator. After 24 hours, MTT (TC191, Himedia) stock solution of 5 mg/ml was added to the wells containing 200µl of media such that the final MTT concentration was 0.5 mg/ml. The cells were then allowed to incubate in dark in the cell-culture incubator for 4 hours and visualized under the microscope for formazan crystals. The media containing MTT were discarded and the formazan-filled cells were dissolved in 100µl of DMSO. Formazan was allowed to solubilize for 15 minutes after which the absorbance was measured in a UV-visible spectrophotometer (Multiscan Go, Thermo Scientific) at 570 nm. All measurements were taken in triplicates. The cell viability was measured using the formula:

$$Cell\ Viability\ \% = \frac{(S - B_S) - (PC - B_{NC})}{(PC - B_{PC}) - (PC - B_{NC})} \times 100 \quad (13)$$

Where S=test sample, B=blanks, PC=positive control, NC=negative control.

3.2. Calculation for affinity constant of aspartame to model membrane

The affinity constant of aspartame to the lipid membrane, knowledge about the cooperativity, as well as the degree of coverage was obtained from the zeta potential information.^{9,10} The protocol followed to extract such information and the useful equations are provided below-

$$\text{Degree of coverage } (\theta) = \frac{\xi_0 - \xi}{\xi_0 - \xi_{max}} \quad (14)$$

In the above equation, ξ_0 indicates the zeta potential of the vesicles in absence of aspartame, ξ_{max} stands for the zeta potential of the vesicle in presence of highest concentration of aspartame, and ξ is the zeta potential of the vesicle in presence of intermediate concentrations of aspartame.

Again, in terms of affinity constant (K) of aspartame to the model membrane, the equation can be written as,¹⁰

$$\text{Degree of coverage } (\theta) = \frac{(KC)^n}{1 + (KC)^n} \quad (15)$$

Here K is the affinity constant, C indicates the concentration of aspartame, and n stands for cooperative coefficient.

Hence, by determining values of θ at different concentration of aspartame, and by plotting $\ln \frac{\theta}{(1-\theta)}$ versus $\ln C$, the value of cooperative coefficient (n), and affinity constant (K) can be determined.

3.3 Estimation of Young's Modulus from nanoindentation experiment: Nanoindentation experiment was performed using the instrument of Model No TI 950 TriboIndenter, Hysitron Inc., USA, fitted with a Berkovich indenter at room temperature. The displacement-controlled indentation cycle was programmed at a penetration depth fixed at 50 nm for the aspartame fibrillar samples, whereas this depth was 200 nm for the reference pure glass. The test cycle time was approximately 10-0-10 seconds for each point. In terms of the experimental part, the sample of the aspartame fibrils was prepared via the drop-casting of the solution of the aspartame of different concentrations on the surface of a glass cover-slip. During the indentation experiment, the attached cantilever of the instrument moved above the samples with a constant force of 10 μN . The locations of the samples were accomplished with the help of an optical microscope. After the extend-retract force curve was recorded, the cantilever retracted and moved to another spot to perform the next cycle. The in-built software attached with the instrument provided the value of the reduced modulus (E_r) as well as hardness. Young's modulus (E) of the samples then was calculated using the following equation¹¹

$$\frac{1}{E_r} = \frac{1 - \nu_s^2}{E} - \frac{1 - \nu_i^2}{E_i} \quad (16)$$

In the above equation, Poisson's ratio (ν_i) and modulus (E_i) of the indented material is 0.07 and 1140 GPa respectively¹¹ and the sample's Poisson ratio is considered as 0.3, as mentioned in earlier literatures for various fibrillar samples.^{12,13}

3.4. Fitting of time-resolved fluorescence anisotropy decays

The fluorescence anisotropy decay $r(t)$ of C-153 was fitted using the equation mentioned below¹⁴–

$$r(t) = a_1 \exp(-t/\tau_{r1}) + a_2 \exp(-t/\tau_{r2}) \quad (17)$$

In the above equation, a_1 and a_2 are the pre-exponential factors connected by $(a_1 + a_2) = r_0$, which is the fundamental anisotropy. On the other hand, τ_r indicates the rotational correlation time. The instrument response function required in the fitting procedure was obtained by substituting the sample with the ground glass scatterer.

4. Supporting tables

Table S1. Average size (Z_{avg}) and polydispersity index (P.D.I) of the solution containing aspartame self-assembled structures after 24 hours of solution preparation

System	$Z_{average}$ (nm) ^a	P.D.I
1.2 mM aspartame	721	0.70
2 mM aspartame	1187	0.846
5 mM aspartame	1245	0.957

^aExperimental error $\pm 5\%$

Table S2. Mechanical parameters of aspartame (ASP) fibrils of various concentrations with reference to the pure glass, obtained from nanoindentation experiment.

System	Hardness	Reduced modulus (E_r)	Young's modulus (E)
Pure glass	7.23	81.80	91
1.2 mM aspartame	0.22	8.51	7.80
2 mM aspartame	0.40	12.36	11.37
5 mM aspartame	1.42	21.47	19.91

Table S3. Zeta potential, ξ (mV) values of DMPC lipid vesicles in absence and presence of various concentrations of aspartame

System	ξ (mV) ^a
Neat vesicle	-22.7
vesicle + 1.2 mM aspartame	-8.03
vesicle + 1.5 mM aspartame	-7.56
Ves + 2 mM aspartame	-6.18
vesicle + 2.5 mM aspartame	-5.17
Ves + 3 mM aspartame	-4.28
Ves + 5 mM aspartame	-2.79

^aExperimental error $\pm 5\%$

Table S4. Average size (Z_{avg}) and FWHM of the sonicated DMPC lipid vesicles in absence and presence of various concentrations of aspartame, as obtained from DLS experiment

System	Z_{avg} (nm) ^a	FWHM of the distribution histogram (nm)
Neat vesicle	114	103
vesicle + 1.2 mM aspartame	120	141
Ves + 2 mM aspartame	118	162
Ves + 5 mM aspartame	122	159

^aExperimental error $\pm 5\%$

Table S5. Time-resolved anisotropy decay parameters of C-153 ($\lambda_{ex} = 400$ nm) in DMPC lipid membranes in the absence and presence of various concentrations of aspartame

System	τ_1 (ns)	τ_2 (ns)	% a_1	% a_2
--------	---------------	---------------	---------	---------

Vesicle	0.52±0.08	3.20 ± 0.32	32%	68%
Vesicle + 5 mM aspartame	0.47±0.06	1.82±0.28	34%	66%

Table S6. Decay parameters of $C(t)$ obtained from solvation dynamics experiment using C-153 ($\lambda_{ex}=400$ nm) within DMPC lipid vesicles in the absence and presence of aspartame

System	τ_1 (ns)	τ_2 (ns)	% a_1	% a_2
Vesicle	0.65±0.03	2.80 ± 0.18	32%	68%
Vesicle + 5 mM aspartame	0.61±0.08	1.60±0.21	34%	66%

Table S7. The values of translational diffusion coefficients (D_t , $\mu\text{m}^2 \text{s}^{-1}$) of DCM inside the DMPC lipid membrane in the absence and presence of aspartame

System	τ_D (μs)	D_t ($\mu\text{m}^2 \text{s}^{-1}$)
Vesicle	6278 ± 210	5.30 ± 0.32
Vesicle + 1.2 mM aspartame	5320 ± 310	6.26 ± 0.36
Vesicle + 2 mM aspartame	4032 ± 350	8.26±0.49
Vesicle + 5 mM aspartame	2643±230	12.60±0.70

5. Supporting figures

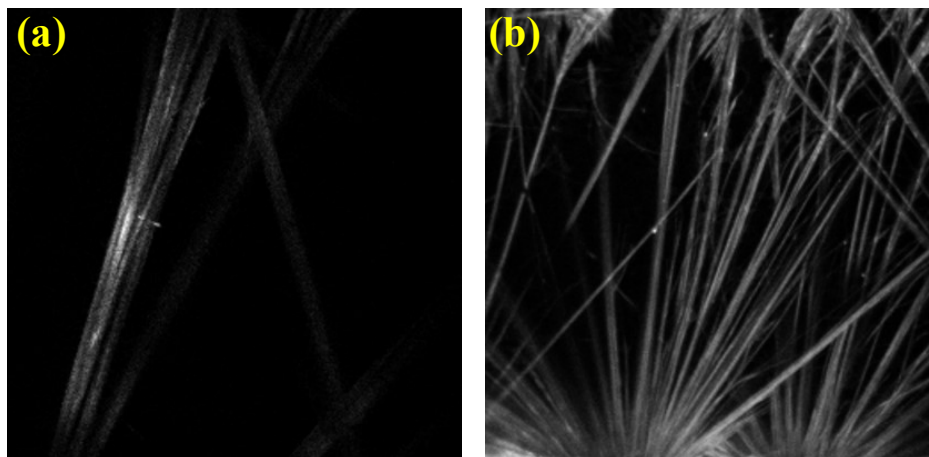


Fig. S1 Intensity mode FLIM images of (a) 1.2 mM and (b) 5 mM aspartame after 24 hours of solution preparation.

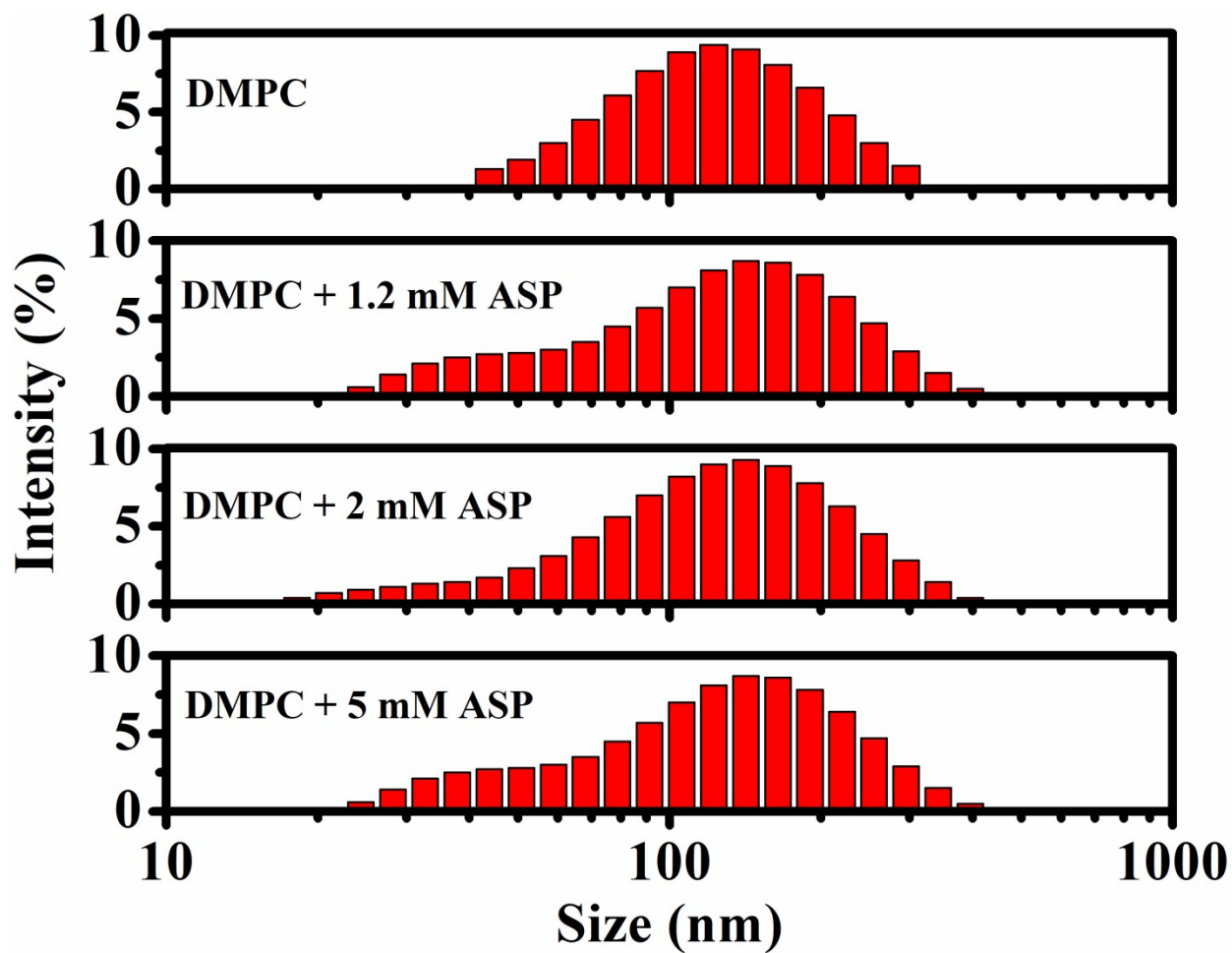


Fig. S2 Intensity-weighted size distribution histogram of aspartame (ASP) fibrils of different concentrations after 24 hours of preparation, obtained from DLS experiment. ($[\text{ASP}] = 1.2 - 5$ mM). Error of triplicate measurements = $\pm 5\%$

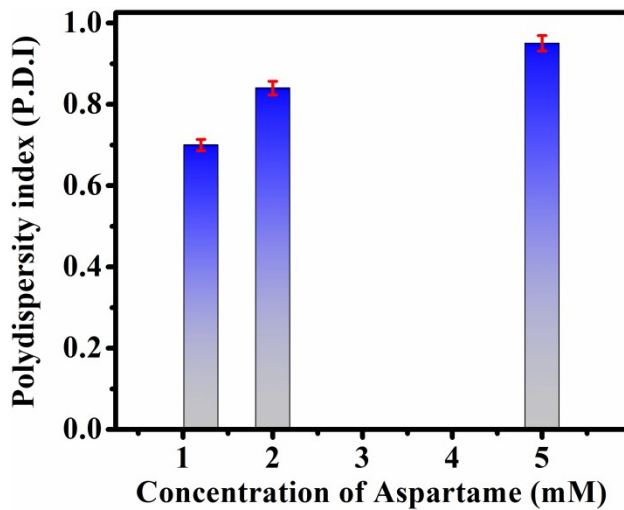


Fig. S3 Measure of polydispersity index (P.D.I) of the aspartame solution as a function of concentration of the aspartame, as obtained from dynamic light scattering experiment. A triplicate mode of measurement shows the error of 2%, as shown by the error bars.

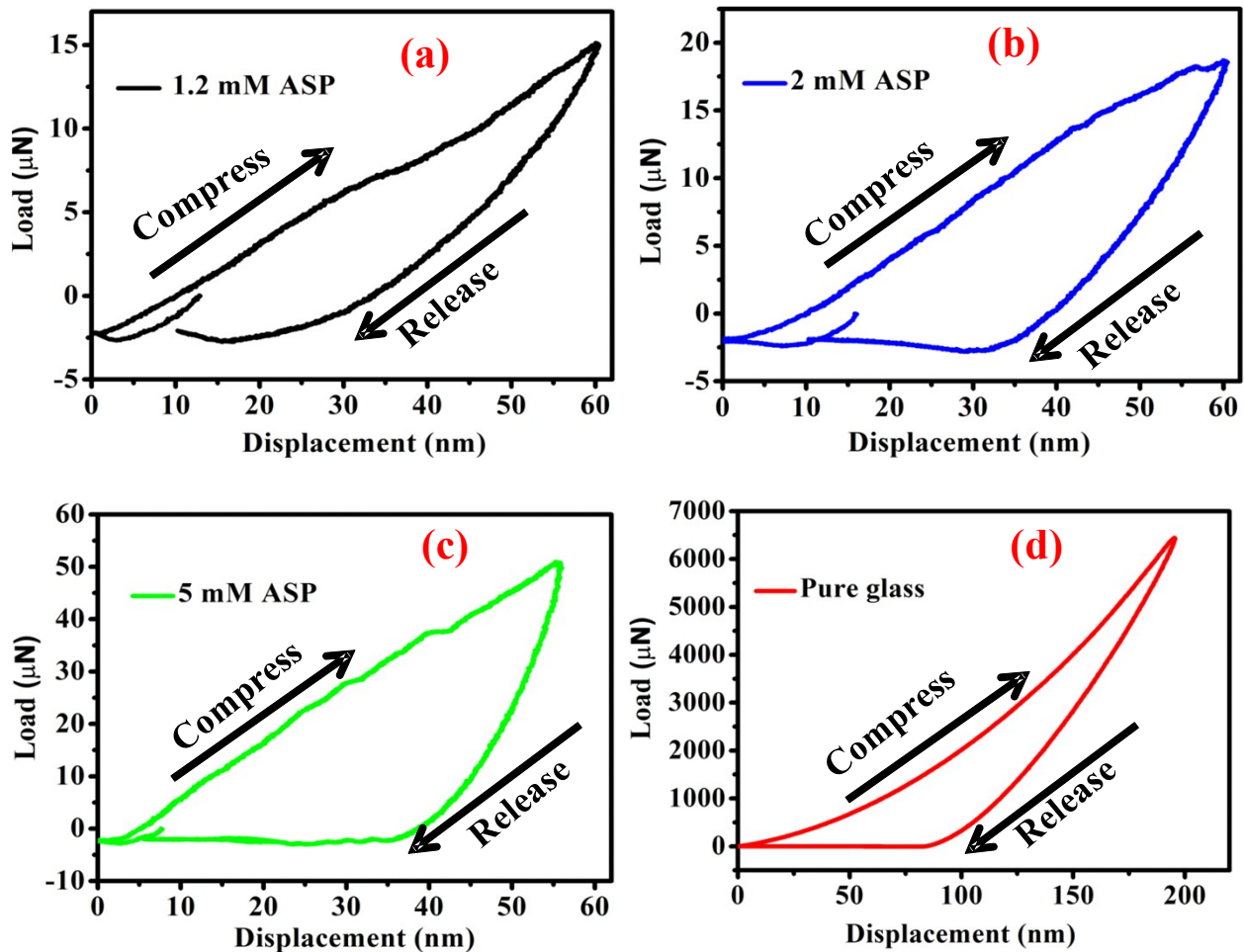


Fig. S4 The plots for load versus displacement obtained from nanoindentation experiment for pure glass and aspartame (ASP) at different concentrations. ($[\text{ASP}] = 1.2, 2, \text{ and } 5 \text{ mM}$, error $\pm 5\%$)

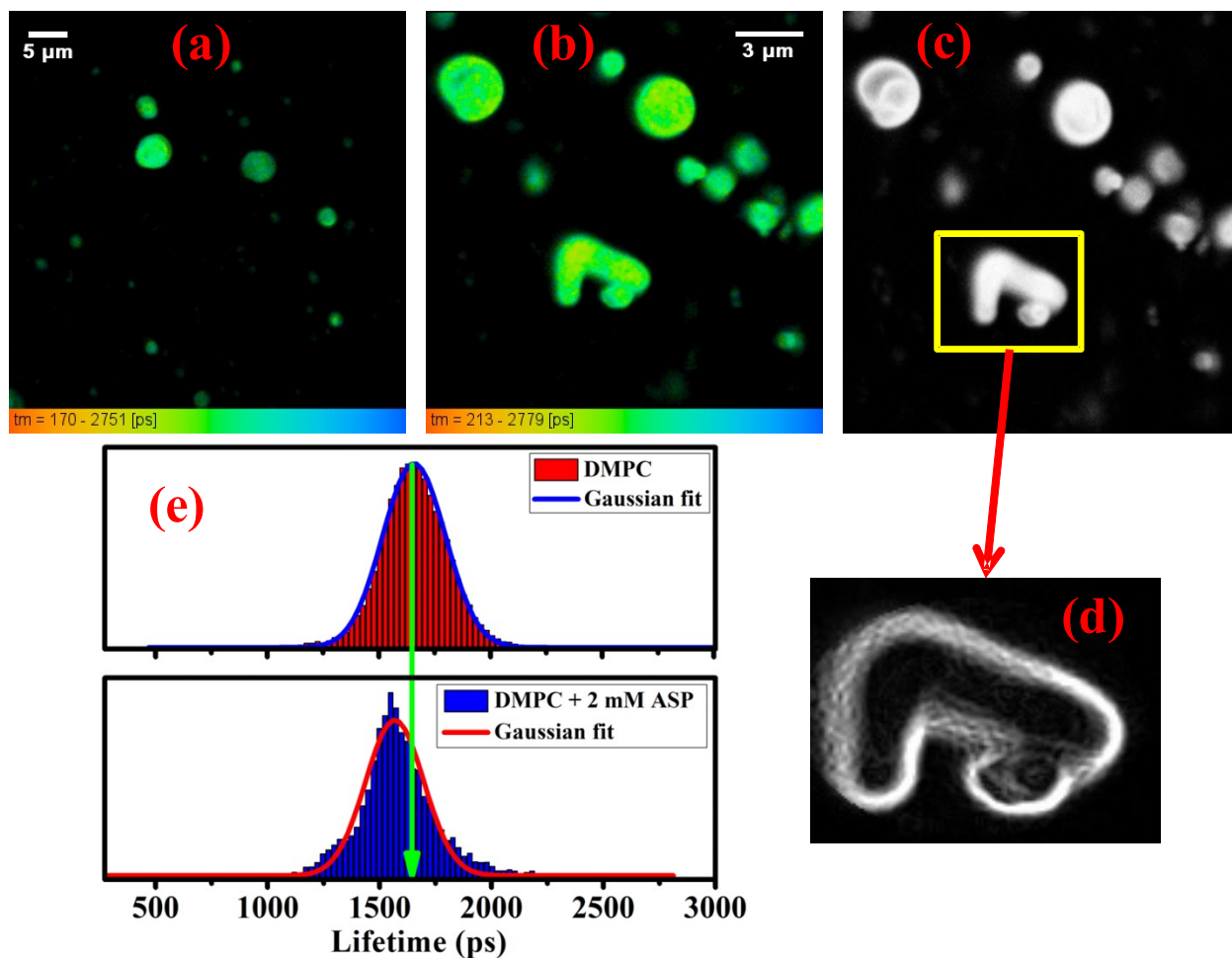


Fig. S5 DCM-stained FLIM images of neat DMPC vesicles (a), DMPC vesicles in presence of 2 mM ASP (b), and its corresponding intensity image (c), where the yellow boxed region of interest has been processed by ImageJ software to clarify the surface contour (d). Fluorescence lifetime distribution of the DCM dye followed by Gaussian fitting for neat DMPC vesicles (central lifetime = 1657 ± 16 ps) and DMPC vesicles in presence of 2 mM ASP (central lifetime = 1560 ± 20 ps) (e).

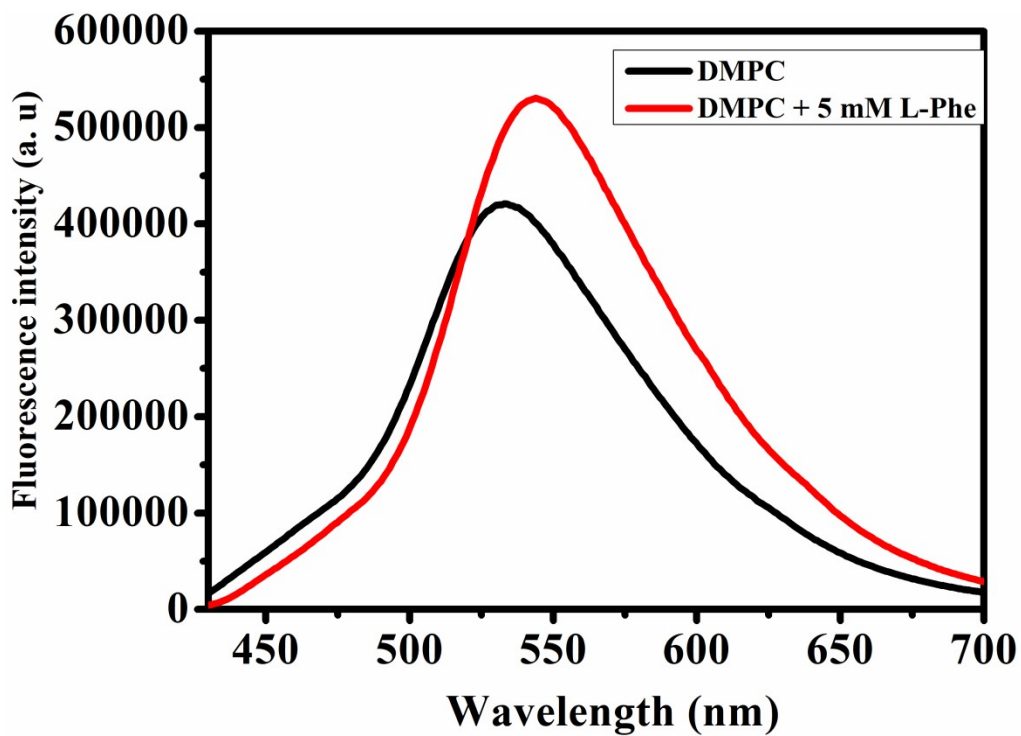


Fig. S6 Steady-state fluorescence emission spectra of C-153 ($\lambda_{\text{ex}} = 400$ nm) in DMPC vesicles in absence and presence of L-Phenylalanine (L-Phe). ($[\text{DMPC}] = 3$ mM, $[\text{L-Phe}] = 5$ mM). Error = ± 3 %.

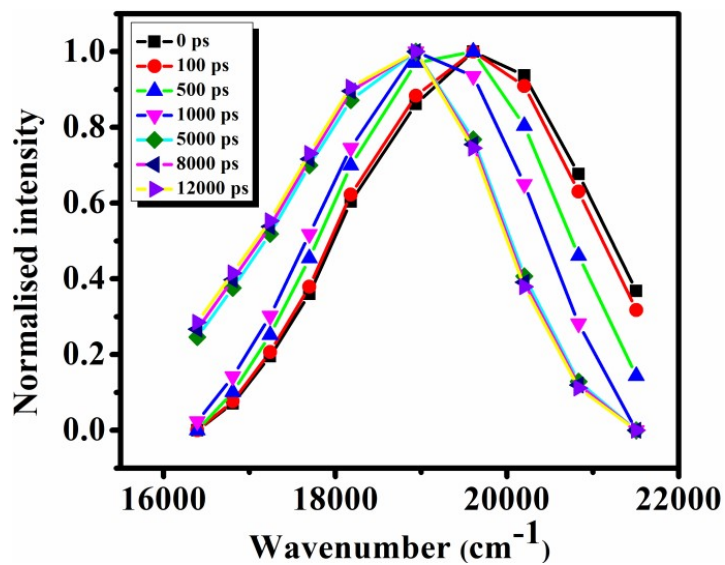


Fig. S7 Time-resolved emission spectra (TRES) of C-153 in the neat DMPC lipid vesicles, as obtained from solvation dynamics experiment. ([DMPC] = 3 mM, λ_{ex} = 400 nm, [C-153] = 3×10^{-5} M).

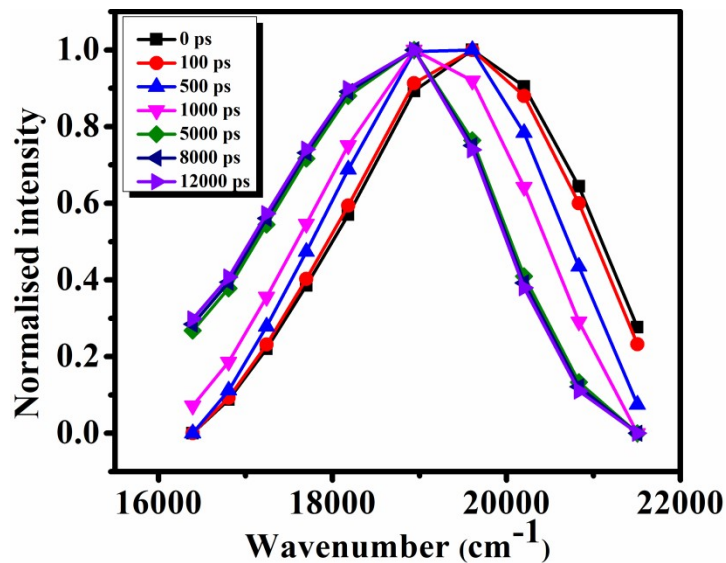


Fig. S8 Time-resolved emission spectra (TRES) of C-153 in the DMPC lipid vesicles containing 5 mM of aspartame, as obtained from solvation dynamics experiment. ([DMPC] = 3 mM, [ASP] = 5 mM, λ_{ex} = 400 nm, [C-153] = 3×10^{-5} M).

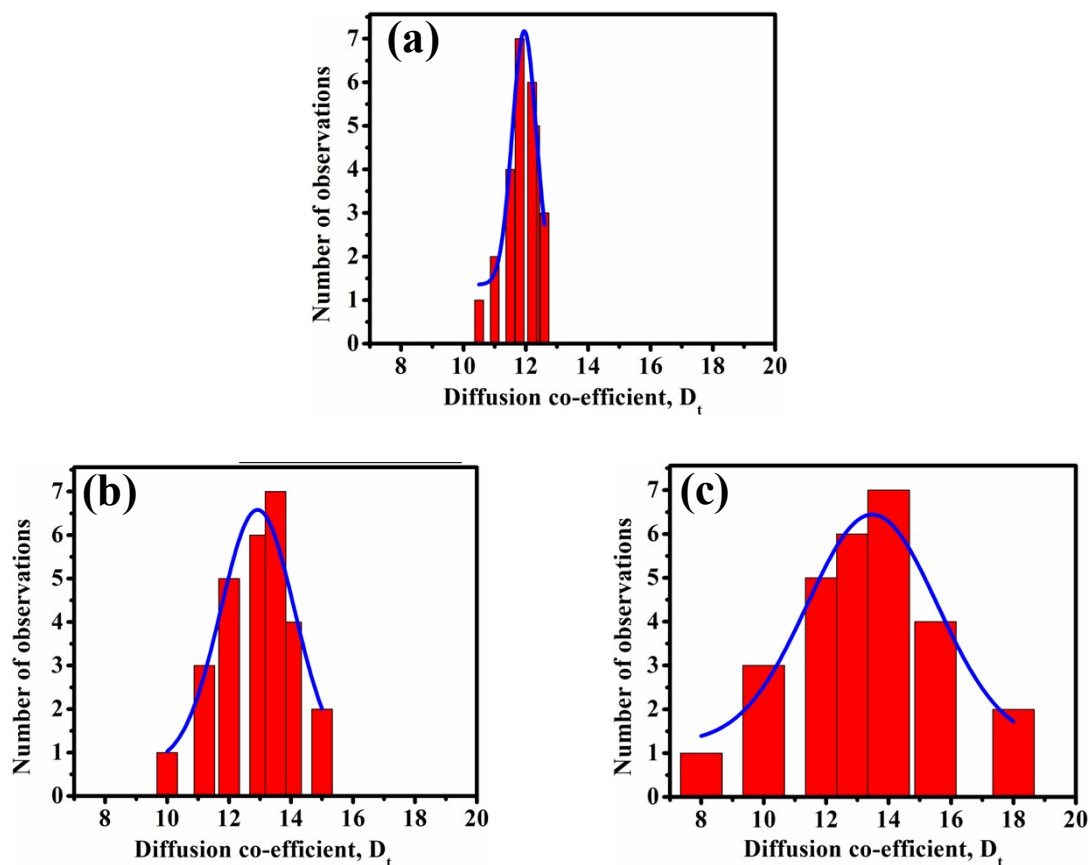


Fig. S9 Distribution of the diffusion coefficient of DCM over seven consecutive measurements in DMPC vesicles containing (a) 1.2 mM, (b) 2 mM, and (c) 5 mM of aspartame. ($[DMPC] = 3$ mM, $[aspartame] = 1.2, 2, 5$ mM, $\lambda_{ex} = 488$ nm).

6. References

1. R. Rigler, U. Mets, W. Widengren, and P. Kask, *Eur. Biophys. J.* 1993, **22**, 169.
2. O. Krichevsky, and G. Bonnet, *Rep. Prog. Phys.* 2002, **65**, 251–297.
3. J. Korlach, P. Schwille, W. W. Webb, and G. W. Feigenson, *Proc. Natl. Acad. Sci. USA.* 1999, **96**, 8461–8466.
4. P. Kapusuta, *Picoquant* 2010.
5. R. Gorenflo, F. Mainardi, D. Moretti, G. Pagnini, and P. Paradisi, *Chem. Phys.* 2002, **284**, 521–541.

6. N. Kundu, P. Banerjee, S. Kundu, R. Dutta, and N. Sarkar, *J. Phys. Chem. B* 2017, **121**, 24–34.
7. M. Maroncelli, and G. R. Fleming, *J. Chem. Phys.* 1987, **86**, 6221–6239.
8. J. R. Lakowicz, 3rd ed. Springer: New York, 2006.
9. A. S. Rosa, A. C. Cutro, M. A. Frías, and E. A. Disalvo, *J. Phys. Chem. B*, 2015, **119**, 15844–15847.
10. E. A. Disalvo, and A. M. Bouchet, *Colloids and Surfaces A: Physicochem. Eng. Aspects*. 2014, **440**, 170–174.
11. P. Banerjee, K. Rajak, P. K. Nandi, S. Pal, M. Ghosh, S. Mishra, and N. Sarkar, *J. Phys. Chem. Lett.* 2020, **11**, 20, 8585–8591.
12. W. Ji, B. Xue, Z. A. Arnon, H. Yuan, S. Bera, Q. Li, D. Zaguri, N. P. Reynolds, H. Li, Y. Chen, S. Gilead, S. Rencus-Lazar, J. Li, R. Yang, Y. Cao, and E. Gazit, *ACS Nano*, 2019, **13**, 14477-14485.
13. L. L. del Mercato, G. Maruccio, P. P. Pompa, B. Bochicchio, A. M. Tamburro, R. Cingolani, and R. Rinaldi, *Biomacromolecules*, 2008, **9**, 796–803.
14. Indirapriyadharshini, V. K.; Ramamurthy, P. Fluorescence Anisotropy of Acridinedione Dyes in Glycerol: Prolate Model of Ellipsoid. *J. Chem. Sci.*, **2007**, *119*(2), 161–168.